



## Di- and tetracarboxylic aromatic acids with silane spacers and their copper complexes: Synthesis, structural characterization and properties evaluation



Maria Cazacu<sup>a,\*</sup>, Angelica Vlad<sup>a</sup>, Mirela-Fernanda Zaltariov<sup>a</sup>, Sergiu Shova<sup>a</sup>,  
Ghenadie Novitchi<sup>b</sup>, Cyrille Train<sup>b, c, d</sup>

<sup>a</sup> “Petru Poni” Institute of Macromolecular Chemistry, Aleea Gr. Ghica Voda 41A, 700487 Iasi, Romania

<sup>b</sup> Laboratoire National des Champs Magnétiques Intenses, CNRS UPR 3228, 25 Rue des Martyrs, 38042 Grenoble, France

<sup>c</sup> Université Joseph Fourier, F-38041 Grenoble, France

<sup>d</sup> Institut Universitaire de France (IUF), 103, bd Saint-Michel, F-75005 Paris, France

### ARTICLE INFO

#### Article history:

Received 10 July 2014

Received in revised form

28 September 2014

Accepted 2 October 2014

Available online 13 October 2014

#### Keywords:

Copper complexes

Dicarboxylic acids

Tetracarboxylic acids

Phenanthroline

2D structures

Hydrogen bonds

### ABSTRACT

Two polycarboxylic acids, bis(*p*-carboxyphenyl)diphenylsilane and bis(3,4-dicarboxyphenyl)dimethylsilane, were prepared according to published procedures and characterized, besides elemental and spectral analysis, for the first time by X-ray single crystal diffraction. Their copper(II) complexes were obtained in the presence of 1,10-phenanthroline as co-ligand, the crystallographic data revealing the formation of 2D structures through hydrogen bonds. The hydrogen bond dynamics of the copper complexes was studied by FTIR-ATR spectrometry. The thermal stability of the acids and derived copper complexes was evaluated by thermogravimetric analysis. The moisture uptake capacity and porosity of the complexes were estimated on the basis of the water vapour sorption measurements in dynamic regime. Magnetic measurements performed on the two metal complexes correspond to not interacting copper(II) with  $S = 1/2$  and  $g$  factor equal to 2.14 and 2.19 being consistent with pentacoordinated Cu(II) paramagnetic centres.

© 2014 Elsevier B.V. All rights reserved.

### Introduction

Polycarboxylic acids are among the most attractive building blocks for the metal-organic frameworks, due to their versatile binding features [1] as well as their robustness and thermal stability [2]. The carboxylate anions which are characterized by an increased electron density on the oxygen atoms, high proton affinity, and low ionization energies are widely used as bridging ligands in polynuclear complexes of *d* elements [3]. The multiple oxygen donors can adopt different coordination modes permitting the formation of the networks with various topologies [4]. The coordination modes of carboxylate ligands are diverse: *syn*–*syn*, *syn*–*anti* or *anti*–*anti* [3]. Carboxylic acids themselves are able to coordinate the metal ions monodentate, preserving the nonionized carboxy group and thus creating conditions for intermolecular hydrogen bonding that leads to supramolecular systems [3]. Thus, carboxylate ligands may act as both counteranions and bridging

ligands to extend the architecture to 1D chains, 2D layer and 3D network [5]. The formation and stability of polynuclear carboxylate complexes, their chemical and physical properties, as well as the tendency to formation of supramolecular systems are in dependence on the acid strength and the donor–acceptor power of the carboxylate ion. These characteristics are affected by the nature of organic group at which the carboxyl group is attached [3]. There are many reports in literature on the using dicarboxylate, tricarboxylate, and tetracarboxylate ligands, which are inter-bridged by mono- or multi-nuclear metal nodes, leading to stable metal-organic frameworks (MOFs) with permanent porosity [1]. Thus, porous structures were built by metal and carboxylate-type ligands, such as phthalate, biphenylcarboxylate, benzenetricarboxylate, and adamantanedicarboxylate or more rigid multicarboxylate ligand such as anthraquinone-1,4,5,8-tetracarboxylic acid [4,6,7]. MOFs with variable dimensionality and different coordination styles have been designed and synthesized in the last time [6–8]. MOFs constructed from tetracarboxylates with rigid spacer groups such as poly(phenylene) or 4,4'-bipyridyl units are also well documented in the literature [1]. Lately, some investigations have been focused on flexible multidentate ligands (malonate [9], 1,4-

\* Corresponding author.

E-mail address: [mcazacu@icmpp.ro](mailto:mcazacu@icmpp.ro) (M. Cazacu).

cyclohexanedicarboxylic acid [10], 1,2,3,4,5,6-cyclohexanehexa carboxylic acid [11], tetrahydrofuran tercarboxylic acid [12], and cyclohexane-1,2,4,5-tetracarboxylic acid [6]), as they are able to form diversified coordination networks with different metal ions [13]. Bis(oxy)isophthalic acid ligands with  $\text{CH}_2$ - and  $(\text{CH}_2)_2$ - spacers, which impart features of flexibility to the tetracarboxylic acid moiety were successfully utilized in the construction of two- and three-dimensional coordination polymers by reacting them with a variety of the oxophilic lanthanoid metal ions [1,2].

In search for new metal-organic framework, in this paper we prepared two polycarboxylic carbosilane acids according to already reported procedures [14–19] but for the first time used as ligands for copper besides 1,10-phenantroline as co-ligand. All involved intermediates and final compounds were structurally characterized. Thermal stability in the solid state and in solution, the moisture behaviour and magnetic properties were evaluated.

## Experimental

### Materials

Diphenyldichlorosilane ( $\text{C}_{12}\text{H}_{10}\text{SiCl}_2$ ) 97%, dimethyldichlorosilane ( $\text{CH}_3)_2\text{SiCl}_2$ ) 98%, 4-bromotoluene ( $\text{C}_7\text{H}_7\text{Br}$ ) 98%, metallic lithium 99%, chromium trioxide ( $\text{CrO}_3$ ) 99.9%, 4-bromo-*o*-xylene ( $\text{C}_8\text{H}_9\text{Br}$ ) 99%, acetic anhydride ( $(\text{CH}_3\text{CO})_2\text{O}$ ) 98%, 1,10-phenantroline ( $\text{C}_{12}\text{H}_8\text{N}_2$ ) 99%, glacial acetic acid ( $\text{C}_2\text{H}_4\text{O}_2$ ) 99.7%, pyridine 99%, copper(II) perchlorate hexahydrate,  $\text{Cu}(\text{ClO}_4)_2 \cdot 6\text{H}_2\text{O}$ , copper(II) sulphate pentahydrate,  $\text{CuSO}_4 \cdot 5\text{H}_2\text{O}$ , anhydrous diethyl ether, *N,N*-dimethylformamide were purchased from Sigma–Aldrich and used as such. Potassium permanganate ( $\text{KMnO}_4$ ), hydrochloric acid ( $\text{HCl}$ ) 35% and sulphuric acid ( $\text{H}_2\text{SO}_4$ ) 96%, ethanol, methanol were received from Chemical Company.

Bis(*p*-tolyl)diphenylsilane (**1**), (*p*-carboxyphenyl)diphenylsilane,  $\text{H}_2\text{L}^1$ , (**2**), bis(3,4-dimethylphenyl)dimethylsilane (**3**) and (3,4-dicarboxyphenyl)dimethylsilane,  $\text{H}_4\text{L}^2$  (**4**) were obtained as described in Supporting information (ESI), according to Refs. [14–19].

### Measurements

Infrared spectra were recorded using a Bruker Vertex 70 FTIR spectrometer in the transmission mode (KBr pellets) between 4000 and  $400\text{ cm}^{-1}$  at room temperature with a resolution of  $2\text{ cm}^{-1}$  and accumulation of 32 scans.

The temperature-dependent ATR-FTIR spectra were recorded in both heating and cooling runs on the Bruker Vertex 70 FT-IR instrument equipped with a Golden Gate single reflection ATR accessory and a temperature controller. The solid samples were added on the ATR crystal surface and sealed with a cap to avoid the solvent evaporation. The temperature varied between 22 and  $52\text{ }^\circ\text{C}$  being increased with  $5\text{ }^\circ\text{C}$  at each registration. After the temperature was changed, the sample was maintained 2 min before the acquisition of the spectrum. The registrations were performed in ATR mode in the  $600\text{--}4000\text{ cm}^{-1}$  spectral range with 64 scans at  $2\text{ cm}^{-1}$  resolution.

ATR-FTIR spectra in solution were registered using a Bruker Vertex 70 FTIR spectrometer equipped with a ZnSe crystal. The measurements were performed in ATR (Attenuated Total Reflectance) mode in the  $600\text{--}4000\text{ cm}^{-1}$  range at room temperature with a resolution of  $4\text{ cm}^{-1}$  and accumulation of 32 scans.

The NMR spectra were recorded on a Bruker Avance DRX 400 MHz Spectrometer equipped with a 5 mm QNP direct detection probe and *z*-gradients. Spectra were recorded in  $\text{CDCl}_3$ , at room temperature. The chemical shifts are reported as  $\delta$  values (ppm).

The electronic absorption spectra were measured with an Analytic Jena SPECORD 200 spectrophotometer in 10 mm optical path quartz cells fitted with polytetrafluoroethylene stoppers.

The thermogravimetric (TG)–differential thermogravimetric (DTG) analysis was performed on a STA 449F1 Jupiter NETZSCH equipment. The measurements were made in the temperature  $20\text{--}700\text{ }^\circ\text{C}$  range under a nitrogen flow ( $50\text{ mL/min}$ ) using a heating rate of  $10\text{ }^\circ\text{C/min}$ . Alumina crucible was used as sample holder.

Dynamic water vapour sorption (DVS) capacity of the samples was determined in the relative humidity (RH) range  $0\text{--}90\%$  by using the fully automated gravimetric analyzer iGAsorp produced by Hiden Analytical, Warrington (UK). The sample was dried at  $25\text{ }^\circ\text{C}$  in flowing nitrogen ( $250\text{ mL/min}$ ) until it reaches a constant weight at  $\text{RH} < 1\%$ . Then, the relative humidity (RH) was gradually increased from 0 to 90%, in 10% humidity steps, each step having a pre-established equilibrium time between 5 and 10 min so as the sorption equilibrium to be achieved every time. When RH decreased, the desorption curves were recorded. The drying of the samples before sorption measurements was carried out at  $25\text{ }^\circ\text{C}$ ,  $35\text{ }^\circ\text{C}$  and  $55\text{ }^\circ\text{C}$  respectively in flowing nitrogen ( $250\text{ mL/min}$ ) until the weight of the sample was in equilibrium at  $\text{RH} < 1\%$ .

Magnetic measurements were carried out on microcrystalline samples of **5** and **6** with a Quantum Design SQUID magnetometer (MPMS-XL). Variable-temperature ( $1.8\text{--}300\text{ K}$ ) direct current (dc) magnetic susceptibility was measured under an applied magnetic field of 0.1 T. All data were corrected for the contribution of the sample holder and diamagnetism of the samples estimated from Pascal's constants [20,21].

Crystallographic measurements for compounds **1**, **2**, **3**, **5**, and **6** were carried out with an Oxford-Diffraction XCALIBUR E CCD diffractometer equipped with graphite-monochromated Mo-*K $\alpha$*  radiation. The crystals were placed 40 mm from the CCD detector. The unit cell determination and data integration were carried out using the CrysAlis package of Oxford Diffraction [22]. All the structures were solved by direct methods using Olex2 [23] software with the SHELXS structure solution program and refined by full-matrix least-squares on  $F_0^2$  with SHELXL-97 [24]. Atomic displacements for non-hydrogen, non-disordered atoms were refined using an anisotropic model. The positional parameters of the  $\text{ClO}_4^-$  anion and solvate DMF molecules for structures **2**, **4** and **5** have been refined as disordered models in combination with the available tools (PART, DFIX, and SADI) of SHELXL97, using anisotropic/isotropic refinement for non-H atoms. The carbon H atoms were placed in fixed, idealized positions and refined as rigidly bonded to the corresponding atom. Hydrogen atoms for OH groups have been placed by Fourier Difference accounting for the hybridization of the supporting atoms and the hydrogen bonds parameters. The molecular plots were obtained using the Olex2 program [23]. The main crystallographic data together with refinement details are summarized in Table 1.

### Procedure

#### Preparation of the copper complex $[\text{Cu}(\text{Bpy})_2(\text{HL}^1)]\text{ClO}_4 \cdot \text{DMF} \cdot \text{H}_2\text{O}$ , **5**

In a 50 mL round bottom flask equipped with magnetic stirrer, and reflux condenser was introduced 0.1000 g (0.24 mmol) bis(*p*-carboxyphenyl)diphenylsilane, **2**, and 5 mL DMF and the mixture was stirred until dissolved. A solution consisting in 0.1698 g (0.94 mmol) 1,10-phenantroline and 5 mL DMF was dropped over this and the resulted mixture was stirred at room temperature for 3 h. After that, another solution formed from 0.1747 g (0.47 mmol) copper perchlorate and 5 mL methanol was added and the stirring continued for 2 h at  $60\text{ }^\circ\text{C}$ . A crystalline product (**5**) was formed within about two weeks. Yield: 0.079 g (79%).

**Table 1**  
Crystallographic data, details of data collection and structure refinement parameters for **1–3, 5** and **6**.

	<b>1</b>	<b>2</b>	<b>3</b>	<b>5</b>	<b>6</b>
Empirical formula	C <sub>26</sub> H <sub>24</sub> Si	C <sub>32</sub> H <sub>34</sub> N <sub>2</sub> O <sub>6</sub> Si	C <sub>18</sub> H <sub>24</sub> Si	C <sub>53</sub> H <sub>44</sub> ClCuN <sub>5</sub> O <sub>10</sub> Si	C <sub>48</sub> H <sub>52.5</sub> CuN <sub>6</sub> O <sub>14.25</sub> Si
Formula weight	364.54	570.70	268.46	1038.01	1033.09
Temperature/K	293	293	200	200	150
Crystal system	Monoclinic	Monoclinic	Orthorhombic	Triclinic	Triclinic
Space group	C2/c	C2/c	Cmc2 <sub>1</sub>	P-1	P-1
a/Å	18.479(5)	16.5947(11)	21.9562(12)	10.270(5)	13.619(2)
b/Å	7.191(5)	7.5485(5)	12.4173(7)	13.941(5)	14.309(2)
c/Å	16.359(5)	25.2409(14)	5.8118(4)	17.906(5)	15.720(2)
α/°	90	90	90	97.419(5)	96.512(5)
β/°	100.842(5)	95.041(6)	90	90.825(5)	109.869(5)
γ/°	90	90	90	93.897(5)	117.951(5)
V/Å <sup>3</sup>	2135.0(17)	3149.6(3)	1584.51(17)	2535.6(17)	2403.9(6)
Z	4	4	4	2	2
D <sub>calc</sub> /mg/mm <sup>3</sup>	1.134	1.204	1.125	1.360	1.427
μ/mm <sup>-1</sup>	0.117	0.119	0.134	0.570	0.554
Crystal size/mm <sup>3</sup>	0.05 × 0.05 × 0.2	0.05 × 0.05 × 0.10	0.10 × 0.01 × 0.20	0.10 × 0.10 × 0.20	0.20 × 0.10 × 0.05
θ min, θ max (°)	5.08–52	4.92–51.98	6.46–52	5.12–52	4.88–52
Reflections collected	4746	6375	3738	30,413	24,060
Independent reflections	2092 [R <sub>int</sub> = 0.0346]	3098 [R <sub>int</sub> = 0.0685]	1203 [R <sub>int</sub> = 0.0515]	9946 [R <sub>int</sub> = 0.0541]	9417 [R <sub>int</sub> = 0.0461]
Data/restraints/parameters	2092/0/124	3098/0/195	1203/1/104	9946/23/636	9417/11/630
R <sub>1</sub> <sup>a</sup> (I > 2σ(I))	0.0672	0.0709	0.0673	0.0645	0.0512
wR <sub>2</sub> <sup>b</sup> (all data)	0.1498	0.1486	0.1772	0.1709	0.1321
GOF <sup>c</sup>	1.018	0.966	1.048	1.044	1.041
Δρ <sub>max</sub> and Δρ <sub>min</sub> /e/Å <sup>3</sup>	0.22/–0.14	0.19/–0.18	0.60/–0.29	0.83/–0.66	1.06/–0.72

<sup>a</sup>  $R_1 = \sum |F_o| - |F_c| / \sum |F_o|$ .

<sup>b</sup>  $wR_2 = \{ \sum [w(F_o^2 - F_c^2)^2] / \sum [w(F_o^2)] \}^{1/2}$ .

<sup>c</sup>  $GOF = \{ \sum [w(F_o^2 - F_c^2)^2] / (n - p) \}^{1/2}$ , where  $n$  is the number of reflections and  $p$  is the total number of parameters refined.

Elem. anal., wt%: Found 60.96; H 4.49; N 6.35. Calcd. for C<sub>53</sub>H<sub>44</sub>ClCuN<sub>5</sub>O<sub>10</sub>Si ( $M = 1038.01$  g/mol): C 61.27; H 4.24; N 6.74.

IR,  $\nu_{\max}$  (KBr), cm<sup>-1</sup>: 391w, 406w, 430w, 470m, 509m, 532m, 543m, 622s, 649m, 663m, 676m, 702s, 725vs, 761w, 771w, 792w, 802w, 846s, 914w, 968w, 997m, 1016m, 1091vs, 1149m, 1184w, 1253m, 1265m, 1313m, 1344m, 1386s, 1429s, 1454w, 1460w, 1517s, 1537s, 1552w, 1583s, 1670s, 1718s, 1940vw, 2003vw, 2611vw, 2775vw, 2854w, 2925w, 3022w, 3068w, 3415s, 3653vw (Fig. 1Sc).

UV–VIS (DMF):  $\lambda_{\max} = 330$  nm ( $\epsilon = 486$  mol<sup>-1</sup> cm<sup>-1</sup>);  $\lambda_{\max} = 344$  nm ( $\epsilon = 248$  mol<sup>-1</sup> cm<sup>-1</sup>);  $\lambda_{\max} = 443$  nm ( $\epsilon = 126$  mol<sup>-1</sup> cm<sup>-1</sup>) (Fig. 7S).

#### Preparation of the copper complex [Cu(Bpy)<sub>2</sub>(H<sub>2</sub>L<sup>2</sup>)]<sub>2</sub>DMF·4.25 H<sub>2</sub>O, **6**

0.1287 g (0.51 mmol) copper sulphate pentahydrate was dissolved in 3 mL DMF in a 50 mL round bottom flask equipped with magnetic stirrer. Then, a solution consisting in 0.1000 g (0.25 mmol) bis(3,4-dicarboxyphenyl)dimethylsilane, **4**, dissolved in 5 mL DMF and 1 mL distilled water was added over this from a dropping funnel, and the mixture was stirred for two hours. Thereafter, another solution consisting in 0.1855 g (1.030 mmol) 1,10-phenantroline dissolved in 5 mL DMF was dropped. The mixture was stirred 72 h at room temperature after that was filtered. Blue crystals separated from the filtrate after about one month. Yield: 0.089 g (89%). The product is insoluble in THF, CH<sub>2</sub>Cl<sub>2</sub> CHCl<sub>3</sub> but it is soluble in DMF.

Elem. anal., wt%: Found 59.5; H 4.82; N 8.47. Calcd. for C<sub>48</sub>H<sub>44</sub>CuN<sub>6</sub>O<sub>10</sub>Si ( $M = 956.59$  g/mol): C 60.21; H 4.60; N 8.78.

IR,  $\nu_{\max}$  (KBr), cm<sup>-1</sup>: 424m, 489w, 541w, 617s, 682w, 723vs, 769vs, 806s, 827s, 854vs, 1068s, 1105s, 1139m, 1182m, 1224w, 1255m, 1288w, 1313s, 1377vs, 1425vs, 1488m, 1517s, 1585s, 1608vs, 1658vs, 1714s, 2925w, 2958vw, 3060w, 3415s (Fig. 4Sc).

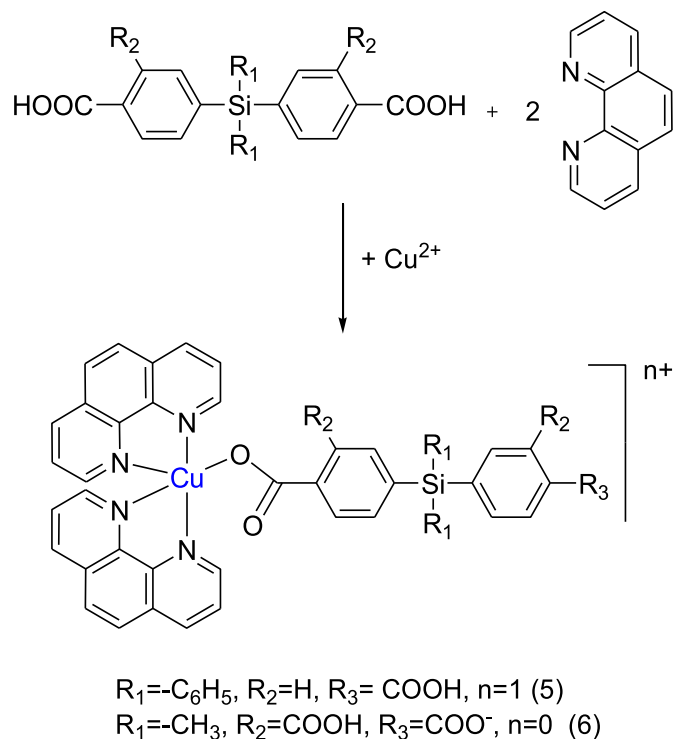
UV–VIS (DMF):  $\lambda_{\max} = 330$  nm ( $\epsilon = 4930$  mol<sup>-1</sup> cm<sup>-1</sup>);  $\lambda_{\max} = 346$  nm ( $\epsilon = 2420$  mol<sup>-1</sup> cm<sup>-1</sup>);  $\lambda_{\max} = 443$  nm ( $\epsilon = 85$  mol<sup>-1</sup> cm<sup>-1</sup>) (Fig. 8S).

## Results and discussion

Two silicon-containing polycarboxylic acids, bis(*p*-carboxyphenyl)diphenylsilane, **2**, and bis(3,4-dicarboxyphenyl)dimethylsilane, **4**, were prepared according to already published multisteps procedures [14–19] (ESI) but for the first time, the main intermediates, **1** and **3**, and finally products **2** and **4**, were structurally characterized by X-ray crystallography, besides common elemental and spectral methods. The carboxylic acids were prepared in view of their use as organic building units for metal-organic frameworks on the assumption that the presence in their structures of the relative flexible spacer, C–Si–C, would facilitate the self-assembling in supramolecular architectures, decrease phase-transition temperatures, and improve solubility. In addition, the phenyl rings can freely rotate around the C–Si–C single bond according to the small change in the coordination environment in order to minimize the steric hindrance [25]. The carboxylic groups can be partially or completely deprotonated, leading to various coordination modes; they can be involved in hydrogen bonds both as an acceptor or a donor while the aromatic ring can stabilize the crystal structure via  $\pi$ – $\pi$  stacking interactions. These structural properties are essential in the design of high dimensional frameworks [26]. Thus, the two carboxylic acids, **2** and **4**, were reacted with copper(II) salt in presence of 1,10-phenantroline as co-ligand when green crystalline complexes, **5** and **6**, respectively were formed (Scheme 1).

#### FTIR analysis

In FTIR spectrum of the complex **5**, the absorption band assigned to deprotonated carboxyl group involved in copper coordination at 1659 and protonated group at 1715 cm<sup>-1</sup> are present. The bands at 424 and 617 cm<sup>-1</sup> are assigned to  $\nu_{M-N}$  and  $\nu_{Cu-O}$ , respectively [27,28]. Similar, in the compound **6**, deprotonated and protonated carboxyl groups are manifested by the presence in IR spectrum of the absorption bands at 1670 and 1719 cm<sup>-1</sup> while the bands assigned to  $\nu_{M-N}$  and  $\nu_{Cu-O}$ , can be identified at 407 and 623 cm<sup>-1</sup>.



**Scheme 1.** Complexation of copper(II) with dicarboxylic/tetracarboxylic acids **2** and **4** in presence of 1,10-phenanthroline leading to compounds **5** and **6**.

### Crystallography

X-ray single-crystal study has revealed that the starting compounds **1** and **3** used to design polycarboxylate ligands exhibit molecular crystal structure built from neutral entities depicted in Figs. 1 and 2, respectively. The Si1 atom in the crystal structure **1** occupies the special position on twofold axis. Because the Si1, C<sub>9</sub> and C<sub>10</sub> atoms in the crystal structure **3** are located on mirror plane, the molecular structure of **1** and **3** compounds is characterized by imposed C<sub>2</sub> and C<sub>s</sub> symmetry, respectively. According to X-ray crystallography, H<sub>2</sub>L<sup>1</sup>·2DMF (**2**) has a molecular structure

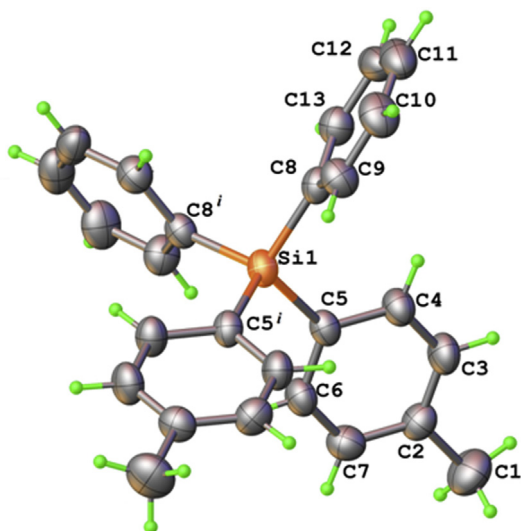


**Fig. 1.** X-ray molecular structure of compound **1**. Thermal ellipsoids are drawn at 30% probability level. Symmetry code for equivalent atoms:  $1 - x, y, 1/2 - z$ .

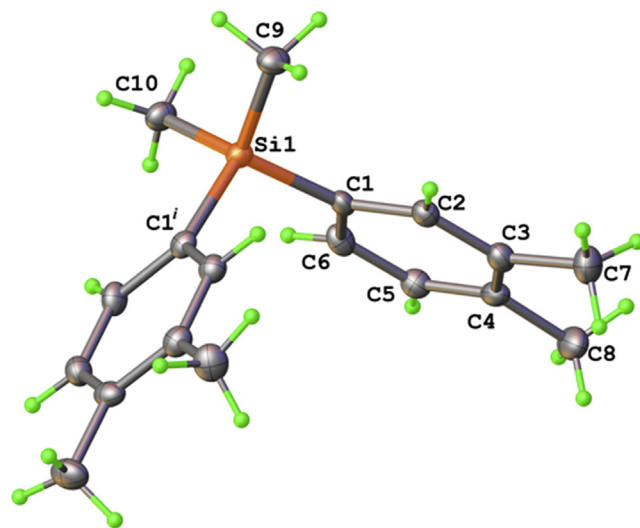


**Fig. 2.** X-ray molecular structure of compound **3**. Thermal ellipsoids are drawn at 30% probability level. Symmetry code for equivalent atoms:  $-x, y, z$ .

consisting from bis(*p*-carboxyphenyl)diphenylsilane and DMF as solvate molecules in 1:2 ratio. Si atom in the H<sub>2</sub>L<sup>1</sup> unit is located on two fold axis which imposed the own C<sub>2</sub> symmetry of the bis(*p*-carboxyphenyl)diphenylsilane molecule. The main crystal structure motif results from the packing of isolated molecular associates formed via O–H···O and C–H···O hydrogen bonds between carboxylate groups of bis(*p*-carboxyphenyl)diphenylsilane and solvate DMF (Fig. 3). The asymmetric part of the unit cell in the crystal structure **5** is depicted in Fig. 4. It comprises [Cu(Bpy)<sub>2</sub>(HL<sup>1</sup>)]<sup>+</sup> coordination cation, ClO<sub>4</sub><sup>−</sup> counter anion and DMF and H<sub>2</sub>O as solvate molecules. The Cu atom exhibits a slightly distorted square-pyramidal N4O coordination environment provided by two bidentate Bpy and monodeprotonated bis(*p*-carboxyphenyl)diphenylsilane ligands. The second carboxylate group is non-deprotonated and does not participate into the coordination to copper atom so that the charge balance is in agreement with the formation of species [Cu(Bpy)<sub>2</sub>(HL<sup>1</sup>)]<sup>−</sup>. The coordination cations are associated in the crystal through O–H···O hydrogen bonds into

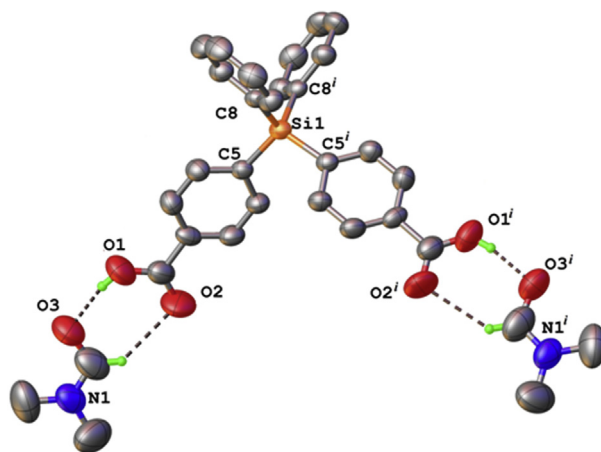


**Fig. 3.** X-ray structure of H<sub>2</sub>L<sup>1</sup> (**2**). Non-relevant H-atoms are omitted for clarity. Thermal ellipsoids are drawn at 50% probability level. Symmetry code:  $1 - x, y, 3/2 - z$ . H-bonds parameters: O1–H···O3 [O1–H 0.82 Å, H···O3 1.69 Å, O1···O3 2.510(7) Å, O1–H···O3 170.5°], C14–H···O2 [C14–H 0.93 Å, H···O2 2.57 Å, C14···O2 3.247(7) Å, C14–H···O2 129.6°].

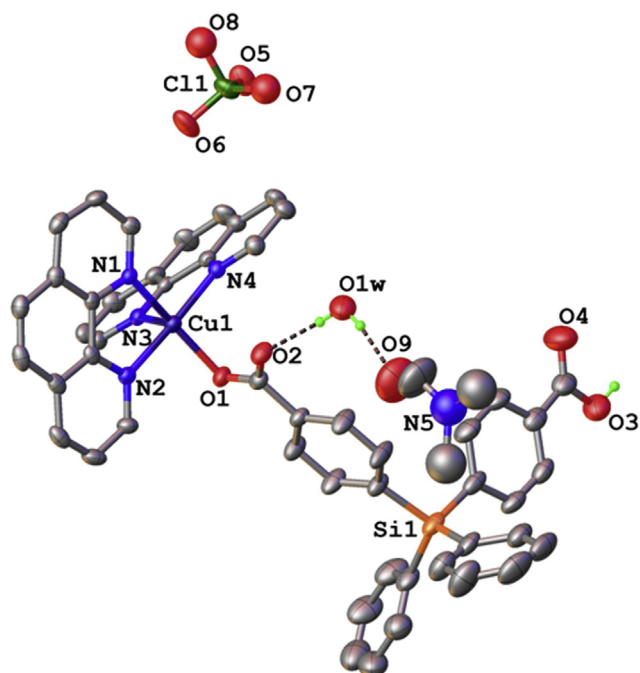


**Fig. 4.** View of the independent part of the unit cell in the crystal structure **5**. Some H-atoms are omitted. Thermal ellipsoids are drawn at 40% probability level. Selected bond lengths (Å) and angles ( $^{\circ}$ ): Cu1–O1 1.953(2), Cu1–N1 2.033(3), Cu1–N2 2.003(3), Cu1–N3 2.205(3), Cu1–N4 2.018(3); O1Cu1N4 91.7(1), O1Cu1N2 91.2(1), O1Cu1N3 96.6(1), N4Cu1N3 79.6(1), N4Cu1N1 95.4(1), N2Cu1N3 100.7(1), N2Cu1N1 81.7(1), N1Cu1N3 101.5(1), O1Cu1N1 161.4(1), N2Cu1N4 177.1(1).

supramolecular centrosymmetric dimers, as shown in Fig. 5. Due to the presence of different fragments which are potential proton donors or proton acceptors, the further extension of the crystal structure occurs via a complex network of O–H $\cdots$ O hydrogen bonds and  $\pi$ – $\pi$  stacking interactions. As the results, the crystal structure **5** is characterized as a 2D supramolecular architecture, the fragment of which is shown in Fig. 6.

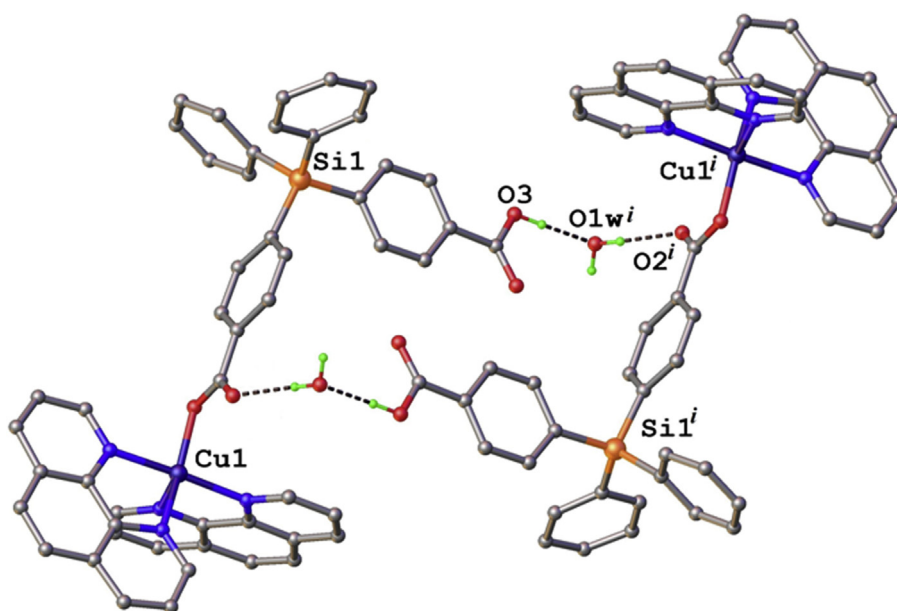


**Fig. 5.** View of H-bonded dimer in crystal structure **5**. Two intramolecular H-bonds O3–H $\cdots$ O1w [O3–H 0.82 Å, H $\cdots$ O1w ( $-x + 1, -y + 1, -z$ ) 1.85 Å, O3 $\cdots$ O1w 2.648(5) Å, O3–H $\cdots$ O1w 163.5 $^{\circ}$ ] and O1w–H $\cdots$ O2 [O1w–H 0.83 Å, H $\cdots$ O2 1.92 Å, O1w $\cdots$ O2 2.741(4) Å, O1w–H $\cdots$ O2 173.7 $^{\circ}$ ] are also shown.

The molecular structure of [Cu(Bpy) $_2$ (H $_2$ L $^2$ )] (**6**) (Fig. 7) resembles in the main the structure of [Cu(Bpy) $_2$ (HL $^1$ )] $^+$  complexation (**5**). In both complexes, the copper atom has a similar coordination polyhedra, where the average Cu–N bond lengths (2.055(2) Å) along with the Cu–O distances (1.986(2) Å) are comparable to those found in earlier studied copper complexes [29]. In contrast to the bis(*p*-carboxyphenyl)diphenylsilane in compound **5**, bis(3,4-dicarboxyphenyl)dimethylsilane, in compound **6**, contains four carboxylate groups, two of them being in deprotonated form. Nevertheless, both carboxylate ligands (HL $^1$  and H $_2$ L $^2$ ) behave as monodentate ligands. As the result, compound **6** has a molecular structure composed from neutral [Cu(Bpy) $_2$ (H $_2$ L $^2$ )] complexes and DMF and water as solvate molecules in 1:2:4.25 ratio. In the crystal, all the components of the structure are assembled by multiple O–H $\cdots$ O hydrogen bonds (Table 2) into two dimensional supramolecular layers, as it is shown in Fig. 8.

#### Hydrogen bond dynamics

The hydrogen bond dynamics of the compounds **5** and **6** have been emphasized by using a FTIR-ATR spectrometer equipped with a temperature controller. The spectra have been recorded from five to five temperature degrees for the both samples during heating until 60  $^{\circ}$ C. In the spectra of the compounds **5** (Fig. 9Sb) and **6** (Fig. 10Sb) recorded during the heating procedure appear the specific broad bands of the OH stretching vibrations at 3731  $\text{cm}^{-1}$  due to dissolution of the hydrogen bonds present in the structure between C=O from acid and water molecules, as it is shown in the molecular structures of the complexes. An important feature of the compounds **5** and **6** is that the structural changes that occur as a result of increasing temperature are reversible. By cooling with the same rate, the initial spectra of the complexes are obtained, indicating that the specific structural hydrogen bonds between carboxylic OH groups and water molecules were reformed.

In order to explain the solubility of the copper complexes, **5** and **6**, a FTIR study was performed in solution (2 mg sample in 0.5 mL DMF) by using ATR-FTIR technique. The solutions containing Cu(II) complexes **5** and **6** were applied on the ZnSe crystal surface and the

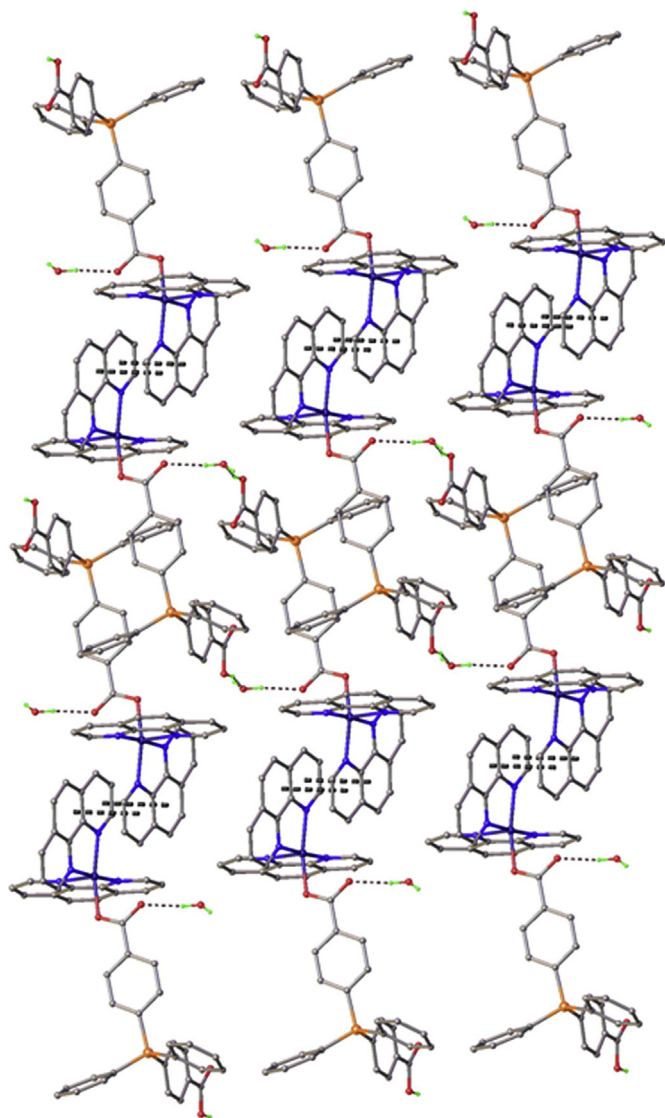


Fig. 6. View of 2D supramolecular layer in the crystal structure 5.

spectra were registered every 5 min until the solvent evaporated, by using repeating measurement experiments at room temperature. Initial, in the FTIR spectra are present the specific bands of DMF ( $2934\text{ cm}^{-1}$  and  $2866\text{ cm}^{-1}$  for methyl groups stretching vibrations,  $1655\text{ cm}^{-1}$  carbonyl-C=O band,  $1256$ ,  $1094$  and  $660\text{ cm}^{-1}$  other specific bands). During the evaporation of DMF, all characteristic bands of the compounds **5** (Figs. 11S) and **6** (Fig. 12S) appear, analogous with the spectra registered in solid state, indicating that the starting structures are reformed.

#### Thermal and moisture behaviour

TG (Fig. 9) and DTG (Fig. 13S) curves were registered for the polycarboxylic acids and their copper complexes in nitrogen atmosphere. Some characteristics extracted from these curves are presented in Table 3. By analysing the thermal data, it can be seen that the decomposition of the dicarboxylic acid, **2**, and derived copper complex, **5**, occurs in four steps while the tetracarboxylic acid, **4**, and its metal complex, **6**, decompose mainly in three steps, the last taking place generally at temperatures greater than dicarboxylates. The higher thermal stability of the compounds **4** and **6**

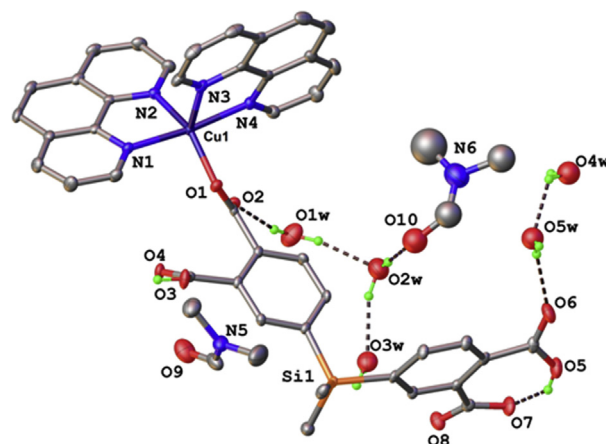


Fig. 7. View of the asymmetric part of the unit cell in the crystal structure  $[\text{Cu}(\text{Bpy})_2(\text{H}_2\text{L}^2)] \cdot 2\text{DMF} \cdot 4.25\text{H}_2\text{O}$ , **6**. Selected bond lengths (Å) and angles ( $^\circ$ ): Cu1–O1 1.986(2), Cu1–N1 2.010(2), Cu1–N2 2.048(2), Cu1–N3 2.194(2), Cu1–N4 2.019(2); O1CuN1 92.08(8), O1CuN2 152.79(9), O1CuN3 98.75(8), O1CuN4 93.43(9), O1CuN2 81.43(9), N1CuN3 95.90(9), N1CuN4 173.4(1), N2CuN3 108.15(9), N4CuN2 95.21(9), N4CuN3 79.72(9).

can be explained by their increased content of aromatic component. The metal complexes proved to be less stable as compared with the corresponding acids. It is possible as the metal to catalyse the decomposition of the complexes [30–32]. This is supported by the less residue amounts in the case of the complexes as compared with carboxylic acids although it would have been expected to be reversed due to the metal presence. However, in all cases, the amount of residue is higher than predicted based on silica and metal content possibly due to formation of the ceramic materials (see ESI).

In the crystal structures **5** and **6**, there are free spaces in the form of 1D channels, the corresponding views of these in desolvated forms being showed in Figs. 18S–20S. These spaces would accommodate different small molecules such as the water that can affect the stability or behaviour of the compounds as environmental moisture changes. Therefore, the *moisture sorption/desorption isotherms* were registered in relative humidity range 0–90%. These are showed in Fig. 10, and some data estimated on their basis are centralized in Table 4. It can notice high differences between the shape of the sorption isotherms and maximum sorption capacities of the two complexes. Thus, the sample **6** shows high hysteresis and increased maximum sorption capacity as compared with sample **5** (i.e., maximum sorption capacity 3.4% for sample **5** and 9.7% for sample **6** at room temperature). Both complexes adsorb more moisture than the acids from which they originate (Fig. 15S) and retain some water (0.5 and 0.6 wt%, respectively) after desorption.

Table 2  
H-bonds parameters for compound **6**.

D–H...A	Distance, Å			Angle D–H...A, deg	Symmetry code
	D–H	H...A	D...A		
O1w–H...O2w	0.86	1.99	2.821(4)	161.6	$x, y, z$
O1w–H...O2	0.87	1.99	2.825(3)	167.9	$x, y, z$
O2w–H...O3w	0.87	1.96	2.794(4)	162.0	$x, y, z$
O2w–H...O10	0.85	1.99	2.836(8)	149.5	$x, y, z$
O–H...O5	0.82	1.79	2.660(3)	173.1	$1 + x, 1 + y, 1 + z$
O3w–H...O8	0.82	2.05	2.864(3)	170.1	$x, y, z$
O4w–H...O5w	0.82	1.82	2.63(1)	169.1	$x, y, z$
O5–H...O7	0.84	1.66	2.376(3)	142.6	$x, y, z$
O5w–H...O6	0.85	2.07	2.864(4)	153.3	$2 - x, 1 - y, 1 - z$
O5w–H...O9	0.85	2.04	2.829(4)	155.0	$2 - x, 1 - y, 1 - z$

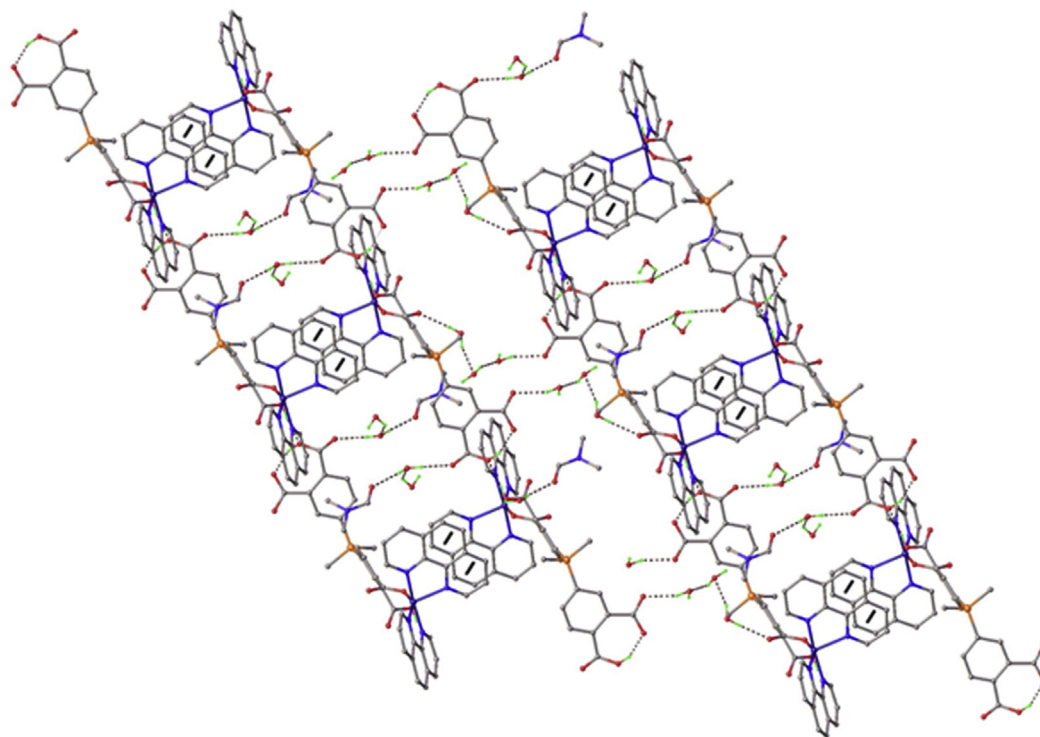


Fig. 8. Two-dimensional supramolecular layer in the crystal structure **6**.

The Brunauer–Emmett–Teller (BET) method [33] was used to evaluate the surface area based on the water vapour sorption data registered in the conditions presented in Experimental section. The sorption values for water activities between 0.05 and 0.35 were considered where BET equation is applicable with good results. The model of Barrett, Joyner and Halenda (BJF model) was applied in order to estimate the average pore size, considering pores to be cylindrical [34]. The method uses the desorption branch of the isotherm. As expected, sample **5** that shows smaller water sorption capacity has larger pores. The results are in agreement with the data estimated on the basis of crystallographic data. The solvent accessible volume determined on the basis of the solvent accessible surface (mapped out by the centre of probe spheres) was calculated based on the structure from which any solvate ( $\text{H}_2\text{O}$  and DMF) molecules were excluded. The technique available in Olex2 [23] by

summarizing the voxels that are at 1.2 Å away from the network substrate was used in this aim. The obtained values are presented in Table 4. It can be seen the higher value of the void volume in the case of sample **6** as compared with **5**.

The differences between maximum sorption values of the two samples determined on the basis of isotherms and their void volumes calculated from crystallographic data are originated probably in the presence of the solvate molecules within the networks that are not completely removed during the drying the sample at 25 °C in nitrogen stream before isotherms registration. In fact, as can be seen from the thermogravimetric data (Fig. 9, Table 3), even by heating up to around 200 °C, the samples did not lose entirely solvent molecules (i.e., DMF) contained within lattice (i.e. samples **5** and **6** loss 5.51 and 10.48 wt% towards a solvate content of 8.78 and 21.55 wt%, respectively as determined by structural analysis).

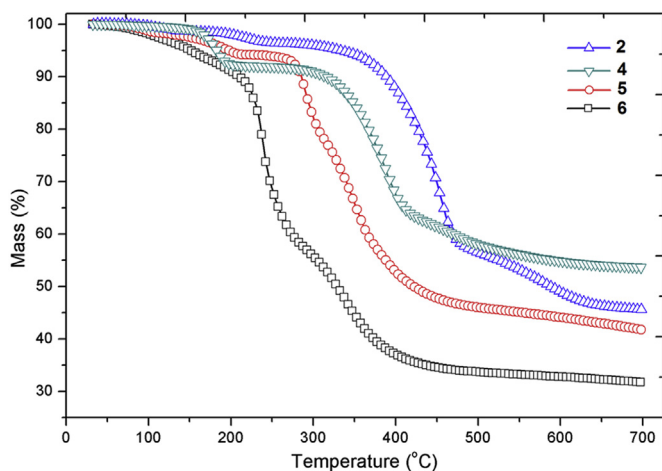


Fig. 9. TGA curves for the carboxylic ligands, **2** and **4**, and metal complexes, **5** and **6**.

Table 3  
The main parameters of the thermograms.

Compound	Peak, step	T (°C)			The mass loss, %	The rest, %
		T <sub>on</sub>	T <sub>max.</sub>	T <sub>of</sub>		
<b>2</b>	I	86.92	102.56	130.47	1.21	45.37
	II	187.33	222.94	237.49	2.30	
	III	342.62	454.17	472.40	37.64	
	IV	~500	581.57	618.17	13.19	
<b>4</b>	I	158.73	184.11	194.19	7.11	53.53
	II	308.9	390.33	406.45	26.93	
	III	~450	465.05	493.43	11.17	
<b>5</b>	I	74.74	96.27	104.39	1.49	41.67
	II	147.15	201.11	208.37	4.02	
	III	275.73	289.23	308.48	16.14	
	IV	321.54	351.95	386.52	36.25	
<b>6</b>	I	80.86	104.6	~200	10.86	31.65
			157.76			
	II	221.10	238.18	268.63	31.23	
	III	308.02	338.46	386.31	25.65	

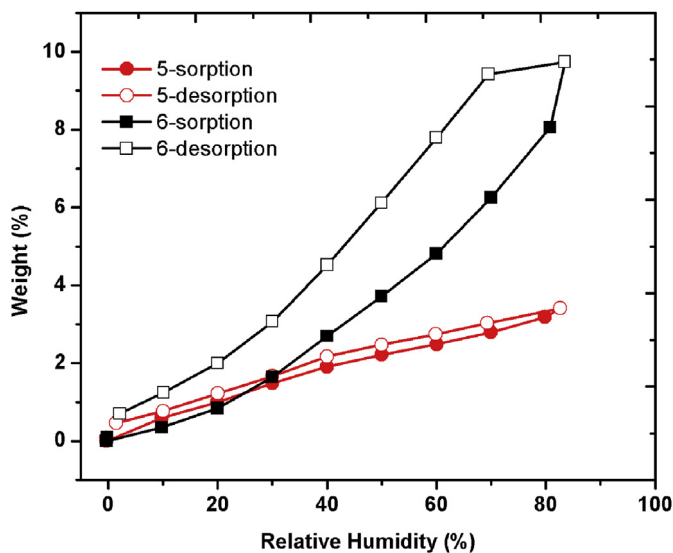


Fig. 10. The shape of the moisture sorption–desorption isotherms for copper complexes **5** and **6** at room temperature.

The sorption values increase as temperature rises; in the same time, the isotherms become more reversible by decreasing the hysteresis loop and water retained after desorption (Figs. 16S and 17S, Table 4).

#### Magnetic properties

Thermal evolution of  $\chi_{MT}$  product of **5** and **6**, is presented in Fig. 11. At room temperature, the  $\chi_{MT}$  product is worth 0.42 for **5** and 0.45 for **6**  $\text{cm}^3 \text{K mol}^{-1}$  which close to the expected  $\chi_{MT}$  value ( $0.375 \text{ cm}^3 \text{K mol}^{-1}$ ) for one isolated  $\text{Cu}^{\text{II}}$  ions ( $d^9$ ,  $g = 2.0$ ,  $S = 1/2$ ) [21]. With decreasing temperature, the  $\chi_{MT}$  product for both compounds remains constant in limit of errors of measurements suggesting absence of any important magnetic interaction. The slightly higher values of  $\chi_{MT}$  should be associated to big  $g$  factor (2.12 for **5** and 2.18 for **6**) of distorted pentacoordinated  $\text{Cu}(\text{II})$  ions. The temperature measurements of magnetic susceptibility are consistent with low temperature magnetisation measurements (Fig. 11). Fits using the Brillouin function with  $S = 1/2$  at 2.0 K indicate  $g = 2.19(1)$  for **6** and  $2.14(1)$  for **5**, which are similar with values obtained from temperature measurements and correspond to non-interacted  $\text{Cu}(\text{II})$  ion.

#### Conclusions

Two new soluble copper(II) complexes were obtained by the reaction of copper salt with well-characterized bis(*p*-carboxyphenyl)diphenylsilane or bis(3,4-dicarboxyphenyl)dimethylsilane

Table 4

The sorption and morphological parameters estimated on the basis of water vapour sorption isotherms and crystallographic data.

Sample	Weight <sup>a</sup> (%d.b.) at			Average pore size <sup>a</sup> (nm)	$A_{\text{BET}}^a$ ( $\text{m}^2/\text{g}$ )	Water accessible volumes <sup>b</sup>	
	25	35	55			$V$ (Å)	$V$ (%)
<b>5</b>	3.4	4.2	6.2	4.41	20.6	493	20.1
<b>6</b>	9.7	12.4	17.1	1.75	110.9	834	34.7

<sup>a</sup> Calculated on the basis of the sorption isotherms.

<sup>b</sup> Estimated based on crystallographic data by using Olex2 technique [23].

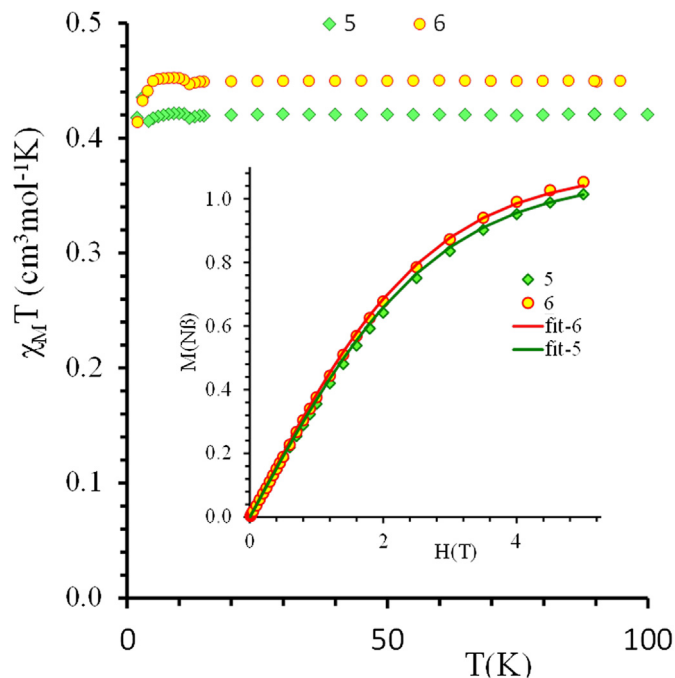


Fig. 11.  $\chi_{MT}$  versus  $T$  plot data for **5** and **6**. Insert figure corresponds to best fits of magnetisation data for **5** and **6** at 2.0 K using Brillouin function.

and 1,10-phenantroline as co-ligands. The crystallographic data revealed the formation of 2D structures through hydrogen bonds, that are destroyed in a reversible way in a polar solvent (DMF) or by heating as FTIR-ATR spectrometry study revealed.

The dicarboxylic acid and derived copper complex, proved to be more thermally stable than tetracarboxylate while the metal complexes were less stable as compared with the corresponding acids. As expected, the tetracarboxylic acid is more hydrophilic than dicarboxylic acid, while the copper complexes absorb more moisture than acids from which they were formed. The moisture sorption capacity increases as temperature rises. The results of the magnetic measurements performed for the two metal complexes correspond to not interacting copper(II) metal centres with  $S = 1/2$  and  $g$  factor equal to 2.14 for **5** and 2.19 for **6**, respectively being consistent with pentacoordinated  $\text{Cu}(\text{II})$  paramagnetic centers.

#### Acknowledgements

This work was supported by a grant of the Ministry of National Education, CNCS – UEFISCDI, project number PN-II-ID-PCE-2012-4-0261. The authors acknowledge to Dr. Olivier Leynaud from Institute NEEL CNRS/UJF UPR2940, Grenoble for powder diffraction X-ray experiments.

#### Appendix A. Supplementary material

CCDC 950973, 950974, 950976, 950977 and 950975 contain the supplementary crystallographic data for this paper. These data can be obtained free of charge from The Cambridge Crystallographic Data Centre via [www.ccdc.cam.ac.uk/data\\_request/cif](http://www.ccdc.cam.ac.uk/data_request/cif).

#### Appendix B. Supplementary data

Supplementary data related to this article can be found at <http://dx.doi.org/10.1016/j.jorganchem.2014.10.006>.

## References

- [1] A. Karmakar, I. Goldberg, *CrystEngComm* 13 (2011) 350.
- [2] A. Karmakar, I. Goldberg, *CrystEngComm* 13 (2011) 339.
- [3] N.S. Panina, A.N. Belyaev, S.A. Simanova, *Russ. J. Gen. Chem.* 72 (1) (2002) 91. Translated from *Zh. Obshch. Khim.* 72 (1) (2002) 98.
- [4] Y. Liu, R. He, F. Wang, C. Lu, Q. Meng, *Inorg. Chem. Commun.* 13 (2010) 1375.
- [5] (a) L.-F. Ma, L.-Y. Wang, F. Zhong, *Synth. React. Inorg. Met.* 38 (2008) 455; (b) D.L. Reger, A. Debreczeni, M.D. Smith, *Inorg. Chem.* 51 (2012) 1068.
- [6] R. Wang, J. Zhang, L. Li, *Inorg. Chem.* 48 (2009) 7194.
- [7] (a) S. Noro, S. Kitagawa, M. Kondo, K. Seki, *Angew. Chem. Int. Ed.* 39 (2000) 2081; (b) Z.L. Huang, M. Drillon, N. Masciocchi, A. Sironi, J.T. Zhao, P. Rabu, P. Panissod, *Chem. Mater.* 12 (2000) 2805; (c) L. Pan, N. Ching, X. Huang, J. Li, *Inorg. Chem.* 39 (2000) 5333; (d) L. Pan, B.S. Finkel, X. Huang, J. Li, *Chem. Commun.* (2001) 105; (e) P.S. Mukherjee, N. Das, Y.K. Kryshchenko, A.M. Arif, P.J. Stang, *J. Am. Chem. Soc.* 126 (2004) 2464; (f) N.L. Rosi, J. Kim, M. Eddaoudi, B. Chen, M. O'Keeffe, O.M. Yaghi, *J. Am. Chem. Soc.* 127 (2005) 1504.
- [8] (a) H. Li, M. Eddaoudi, M. O'Keeffe, O.M. Yaghi, *Nature* 402 (1999) 276; (b) C.J. Kepert, T.J. Prior, M.J. Rosseinsky, *J. Am. Chem. Soc.* 122 (2000) 5158; (c) M. Eddaoudi, J. Kim, N. Rosi, D. Vodak, J. Wachter, M. O'Keeffe, O.M. Yaghi, *Science* 295 (2002) 469; (d) N.L. Rosi, J. Eckert, M. Eddaoudi, D.T. Vodak, J. Kim, M. O'Keeffe, O.M. Yaghi, *Science* 300 (2003) 1127; (e) J.L.C. Rowsell, A.R. Millward, K.S. Park, O.M. Yaghi, *J. Am. Chem. Soc.* 126 (2004) 5666.
- [9] J. Pasan, J. Sanchiz, C. Ruiz-Perez, F. Lloret, M. Julve, *Eur. J. Inorg. Chem.* 20 (2004) 4081.
- [10] W.H. Bi, R. Cao, D.F. Sun, D.Q. Yuan, X. Li, Y.Q. Wang, X.J. Li, M.C. Hong, *Chem. Commun.* (2004) 2104.
- [11] (a) J. Wang, Y.H. Zhang, M.L. Tong, *Chem. Commun.* (2006) 3166; (b) J. Wang, L.L. Zheng, C.J. Li, Y.Z. Zheng, M.L. Tong, *Cryst. Growth Des.* 6 (2006) 357; (c) J. Wang, S. Hu, M.L. Tong, *Eur. J. Inorg. Chem.* (2006) 2069.
- [12] L. Zhang, J. Zhang, Z.J. Li, Y.Y. Qin, Q.P. Lin, Y.G. Yao, *Chem. Eur. J.* 15 (2009) 989.
- [13] (a) M.C. Hong, Y.J. Zhao, W.P. Su, R. Cao, M. Fujita, Z.Y. Zhou, A.S.C. Chan, *J. Am. Chem. Soc.* 122 (2000) 4819; (b) B. Moulton, M.J. Zaworotko, *Chem. Rev.* 101 (2001) 1629; (c) S. Kitagawa, K. Uemura, *Chem. Soc. Rev.* 34 (2005) 109.
- [14] I.K. Varma, K. Chander, R.C. Anand, *Die Angew. Makromol. Chem.* 168 (1989) 217.
- [15] M. Cazacu, A. Airinei, M. Marcu, *Appl. Organomet. Chem.* 16 (2002) 643.
- [16] M. Bruma, E. Hamciuc, B. Schulz, T. Kopnick, Y. Kaminorz, J. Robison, *J. Appl. Polym. Sci.* 87 (2003) 714.
- [17] J.R. Pratt, S.F. Thames, *J. Org. Chem.* 38 (1973) 4271.
- [18] E. Hamciuc, M. Bruma, B. Schulz, T. Köpnick, *High Perform. Polym.* 15 (2003) 347.
- [19] E. Hamciuc, B. Schulz, T. Köpnick, M. Bruma, *High Perform. Polym.* 14 (2002) 63.
- [20] P. Pascal, *Ann. Chim. Phys.* 19 (1910) 5.
- [21] O. Kahn, *Molecular Magnetism*, VCH Publishers, Inc., New York, Weinheim, Cambridge, 1993.
- [22] CrysAlis, Oxford Diffraction Ltd., Version 1.171.34.76, 2003.
- [23] O.V. Dolomanov, L.J. Bourhis, R.J. Gildea, J.A.K. Howard, H. Puschmann, *J. Appl. Crystallogr.* 42 (2009) 339.
- [24] G.M. Sheldrick, *Acta Crystallogr. A* 64 (2008) 112.
- [25] J.-J. Wang, P.-X. Cao, L.-J. Gao, F. Fu, M.-L. Zhang, Y.-X. Ren, X.-Y. Hou, *Chin. J. Struct. Chem.* 30 (2011) 1787.
- [26] Y. Luo, K. Bernot, G. Calvez, S. Freslon, C. Daiguebonne, O. Guillou, N. Kerbellec, T. Roisnel, *CrystEngComm* 15 (2013) 1882.
- [27] J.C. Pessoa, I. Cavaco, I. Correia, M.T. Duarte, R.D. Gillard, R.T. Henriques, F.J. Higes, C. Madeira, I. Tomaz, *Inorg. Chim. Acta* 293 (1999) 1.
- [28] P.T. Ndifon, M.O. Agwara, A.G. Paboudam, D.M. Yufanyi, J. Ngoune, A. Galindo, E. Alvarez, A. Mohamadou, *Transit. Met. Chem.* 34 (7) (2009) 745.
- [29] A. Vlad, M.-F. Zaltariou, S. Shova, G. Novitchi, C.-D. Varganici, C. Train, M. Cazacu, *CrystEngComm* 15 (2013) 5368.
- [30] M. Cazacu, M. Marcu, A. Vlad, A. Toth, C. Racles, *J. Polym. Sci. Part A Polym. Chem.* 41 (20) (2003) 3169.
- [31] M. Cazacu, M. Marcu, A. Vlad, Gh. I. Rusu, M. Avadanei, *J. Organomet. Chem.* 689 (19) (2004) 3005.
- [32] S. Samal, R.R. Das, R.K. Dey, S. Acharya, *J. Appl. Polym. Sci.* 77 (2000) 967.
- [33] S. Brunauer, P.H. Emmett, E. Teller, *J. Am. Chem. Soc.* 60 (1938) 309.
- [34] K.L. Murray, N.A. Seaton, M.A. Day, *Langmuir* 15 (1999) 6728.